BULLETIN OF THE EARTHQUAKE
RESEARCH INSTITUTE
Vol. 36 (1958), pp. 311-327

17. *Seismic Wave Types in a Sand Layer near a Small Explosion.*

By Syun'itiro OMOTE, Shauzow KOMAKI and Naoyoshi NAKAJIMA,

Earthquake Research Institute.

(Read Oct. 25, 1955 and Oct. 23, 1956. — Received June 30, 1958.)

Introduction

We cannot exactly know the nature of the waves of earthquakes by conventional procedures, because these waves are generated under exceedingly complex conditions and are propagated from the hypocentre to observatories through complicated structures of the earth. On the other hand, we know we can study the phenomena of the elastic waves which are generated under ideally simple conditions by means of the model-seismological procedures. But the procedures are so simple that sometimes we cannot apply the result thus obtained to the earthquake. In order to take away the above-mentioned disadvantages, many experimental studies have been carried out in areas having rather simple underground structures to investigate the propagation of the waves produced by an explosion. We may say that we can expect the simplicity of conditions next to that of model seismology in the case of explosion-seismological experiments, and that a full investigation of the observation results obtained in the course of such experiments is useful for the understanding of earthquake phenomena generated in extremely complex conditions.

Because of these considerations, the Seismic Exploration Group of Japan headed by K. Sassa has been carrying out active research along this line since 1953, and is getting fruitful results. As a part of these activities an experiment was carried out on the sand shore of the Japan Sea in Niigata Prefecture by one of the authors with the cooperation of H. Sima and the Research Team of the Japan Petroleum Exploration Co. Ltd., in 1955. The object of the experiment was to promote the study of the generation and the propagation of seismic waves in sand layers near a small explosion. This experiment was supplemented at the same area in the following year, for the purpose of getting some necessary additional data to improve its results.

Experimental procedures

Location

We made experiments in an area on the skirts of dunes, where there was a fairly thick, uniform layer of coarse sand near the surface as illustrated by the core log in Fig. 1. The slant area of the test site

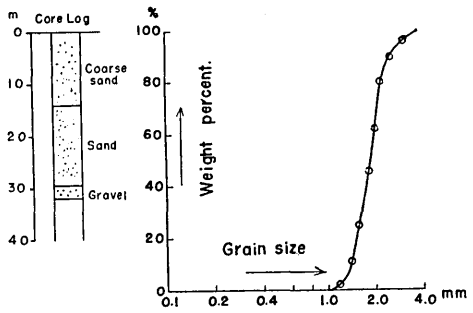

Fig. 1. Sample log and cumulative curve of the coarse sand at the test site.

Table 1. Grain-size distribution of the coarse sand at the test site.

Grain size	Weight percent
>5 mm	0
5~2.5	5.9
2.5~1.2	93.3
1.2~0.6	0.8
<0.6	0

was smooth and of no surface irregularities. The result of the test of grain-size distribution of the coarse sand is tabulated in Table 1 and the cumulative curve of its grain size is steep, as shown in Fig. 1. The area which consists of almost homogeneous and uniform media and has fairly simple underground structures is suitable for seismic experiment by means of a small explosion.

In 1955, as will be described later, the experiment was carried out at a site situated about 20 m away from the brink (Traverse A). Judging from the results of the travel-time curves obtained in the observations, it was certain that there was a plane of discontinuity at about 2.8 m below the surface. This seems to be the boundary plane between the sand layer soaked in sea water and the dry sand layer in view of the topography, because there was no geological discontinuity as shown in the core log. Consequently, it means that we conducted the experiment in 1955 on an area having a half space covered with a horizontal single layer. Naturally, the records thus obtained were not so simple as was expected. In 1956, to carry out a seismic experiment on an ideal uniform half space, we set up a traverse (Traverse B) just along the brink which had one layer consisting of saturated sand at the same site. Moreover, the other traverse (Traverse C) was set up on the same line as in 1955.

Equipment

The equipment used in recording the ground motion was similar to that used commonly in seismic prospecting. E. T. L. geophones, having natural frequencies of 27 cps, were used at each traverse. The output of the geophones was connected to an oscillograph without an amplifier. The galvanometers used in the oscillograph were San-ei's G-100 type, having natural frequencies of 100 cps.

Shooting procedure

In the experiments extending over two years we set up three traverses in all, i.e. A, B and C as shown in Fig. 2. These three traverses were parallel to the straight brink.

Twenty-three vertical geophones were installed along Traverse A at every 25 cm. The epicentral distance spreads from 25 cm to 18 m by removing the shot points. Three-component observations were made at every 75 cm interval.

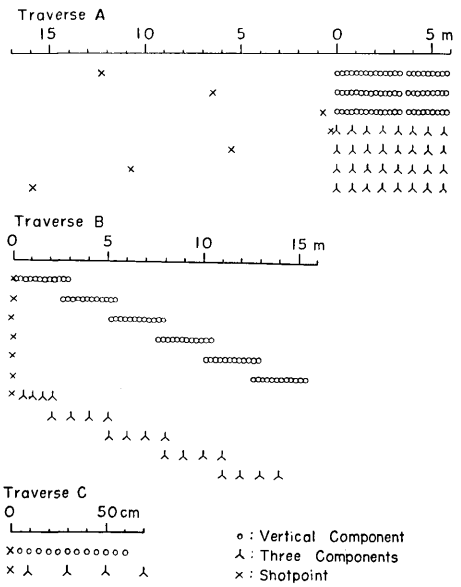

Fig. 2. Location of geophones in the shooting procedure.

Along Traverse B, equipment limitations required the use of several spread segments, with common end geophones, to achieve the desired spread coverage. In this case the shot point was fixed. The space of each geophone in the vertical and the three-component observations was 25 cm and 50 cm respectively.

Similar measurement was carried out on a smaller scale along Traverse C. The interval of each geophone in the vertical and the three-component observations was 5 cm and 20 cm respectively.

As vibration sources we used caps and dynamite in 1955 and caps and carlit in 1956. The charge amount was augmented in proportion to the extent of distance.

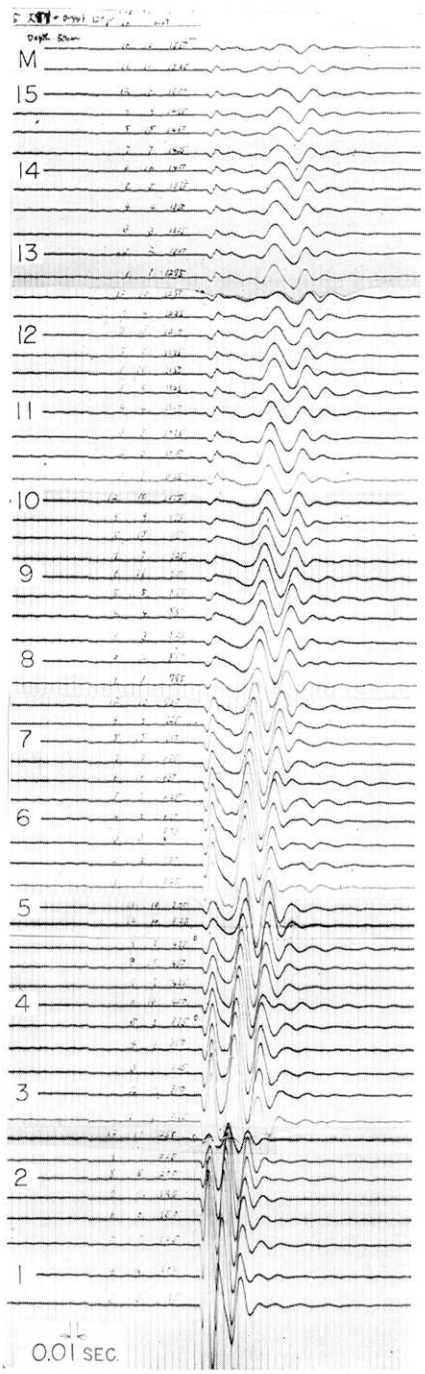

Fig. 3. Typical vertical records obtained along Traverse A.

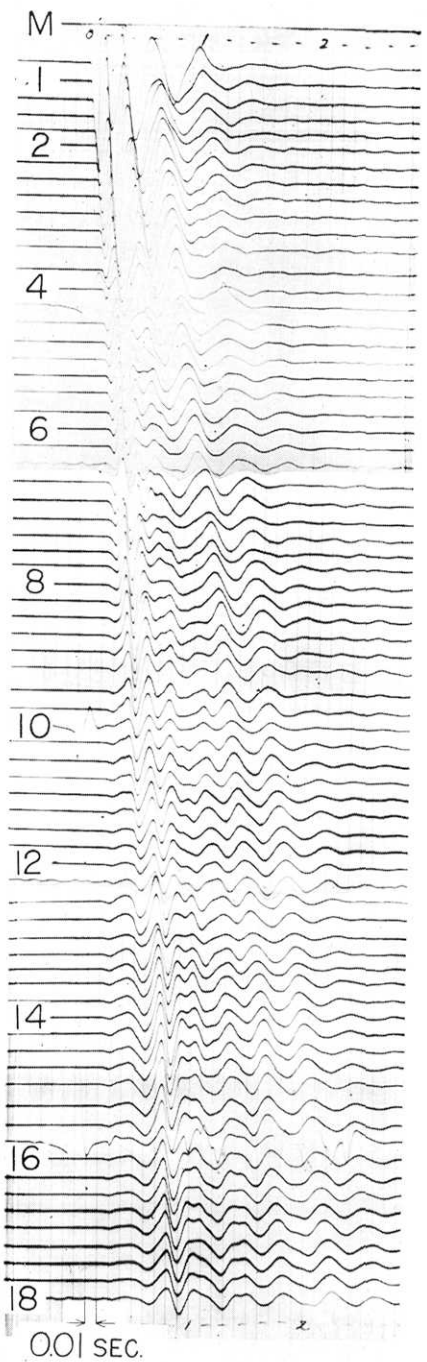

Fig. 4. Typical vertical records obtained along Travese B.

Observed records and travel-time curves

The records of the vertical observations at Traverse A are shown in Fig. 3. The seismograms point out that the experiment has succeeded in getting fairly simple records of small explosions in an area having simple underground structures. The first step in the study of these records was to make travel-time curves. These curves were constructed for all peaks and troughs which had characteristics by which they could be traced. The results on the vertical observations at Traverse A are shown in Fig. 5. This graph will be useful for the classification of wave groups. The slopes of the lines connecting each peak or trough indicate the phase velocities of the respective waves.

In Fig. 5, we have four wave groups having different phase velocities. Roughly speaking, the first wave group shows a similar slope to that of the initial motion at a distance of over 6.5 m. The wave pertaining to this group continues only about half a period. The slope of the second wave group which continues 1∼1.5 periods, is like that of the initial motion at a distance of less than 6.5 m. In another predominant group, i.e. the fourth wave group, the slope is much steeper than those of the two groups, and the duration is 1∼1.5 periods. We find a weak wave group, i.e. the third wave group, between the second and the fourth groups.

Speaking in detail, a train of dots representing the travel-time of peaks or troughs, e.g. II-1U or II-1D, usually do not stand in a straight line, but in the form of the combination of several intermittent lines. That is to say, both the phase velocity and the period of wave gain as the epicentral distance becomes longer. In the second wave group, the phase velocity which shows a value of about 250 m/sec near the shot point amounts to about 350 m/sec and 460 m/sec respectively in the vicinity of 10 m and 15 m from the shot point. Neverthless, the phase velocity of each wave group is given in Table 2 as the mean value of the all phase velocities involved in the group itself. While the period of wave in the second wave group shows values of about 0.013 sec, 0.017 sec and 0.020 sec respectively near the shot point and two other places stated above. The mean values of the period of wave of the four groups are also listed in Table 2 in the same way as those of the phase velocity.

Of these four wave groups, the first one is the bodily P wave propagated through the substratum. The initial arrival and the first peak, i.e. II-1U, of the second wave group represent the bodily P wave

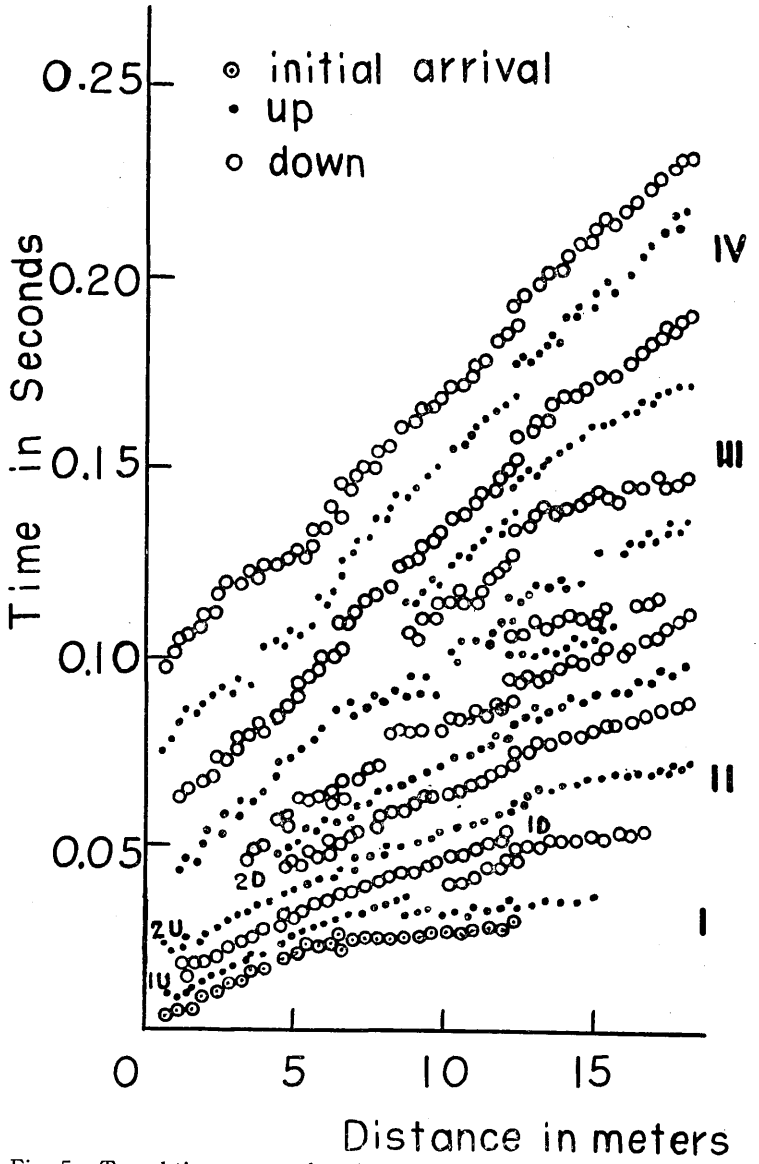

Fig. 5. Travel-time curves for all principal seismic waves observed at Traverse A.

propagated through the superficial layer. On the other hand, the undulation following the initial wave in the same wave group has a dispersive characteristic that the period of wave becomes longer as the phase velocity increases which we have seen in the preceding paragraph.

Table 2. Classification of the wave groups.

Group	Phase velocity	Period
I	1400 m/sec	1.1×10^{-2} sec
II	340	1.6
III	210	2.0
IV	135	3.6

Because of this dispersive characteristic, we considered this part of the waves in the second group as a kind of surface wave. H. Takeuchi and N. Kobayashi[1] had given an opinion that the latter part of the second wave group will be explained as a kind of surface P wave. The third and the fourth wave groups are regarded as surface waves from their dispersive characteristic as in the case of the second wave group.

The travel-time curve from the initial arrival consists of two segments and indicates that the ground structure of the area is not a simple uniform half-space. On the assumption that the ground structure is a half space covered with a horizontal single layer, the depth of the boundary plane is calculated as about 2.8 m. Keeping the topography of the area in mind, it can be concluded that this boundary represents an interface between the dry sand layer and the thick water-soaked sand layer, both of uniform elastic properties, and that the upper layer has a P-phase velocity of 245 m/sec and the lower layer has one of 1400 m/sec which appears to be constant for a spread of distance out to 20 m.

In 1956, in order to conduct the seismic experiment on an ideal uniform half-space, small explosion-seismic observations were made on Traverse B which was set up just along the brink. In this experiment it was reasonablly expected that a superficial overburden of a dry sand layer such as we found in of Traverse A would not be found any longer in Traverse B, because the latter traverse was set up so close to the brink.

The records of the vertical observations on this traverse are illustrated in Fig. 4, arranged in order of epicentral distance. On the basis of these recordes, we made the time-distance plot for all peaks and troughs in the same way as in the case of Traverse A, the result of which is shown in Fig. 6. From this graph it can be seen that the slope of the plot consists of only two groups. The first group has a phase velocity of 1460～1480 m/sec, similar to that of the first group at

1) H. TAKEUCHI and N. KOBAYASHI, *Rep. Seis. Exp. Group of Japan*, **9** (1956), 1, (in Japanese).

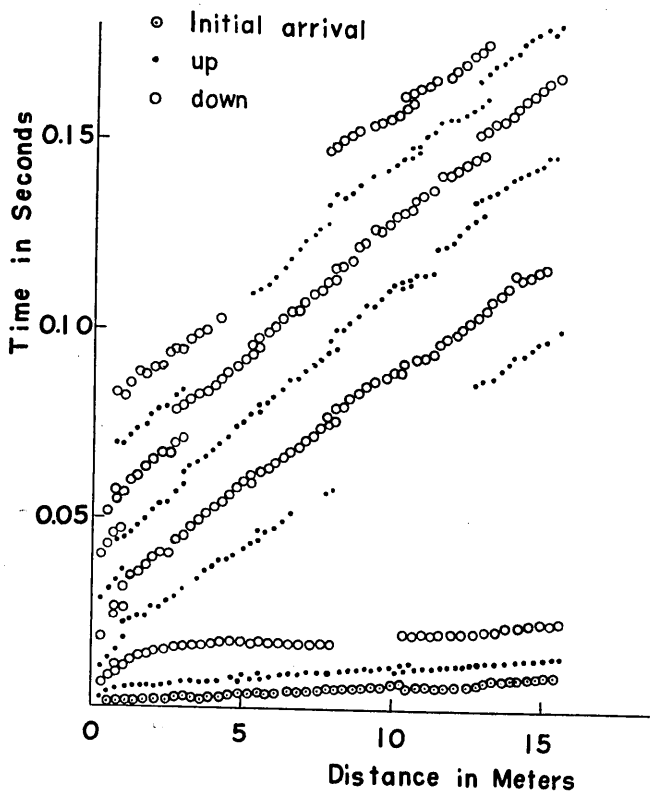

Fig. 6. Travel-time curves for all principal seismic waves observed at Traverse B.

Traverse A and it corresponds to the P wave propagated through the sand layer soaked in sea water. The other group, having a phase velocity of 160~180 m/sec, is regarded as a surface wave in reference to the case of Traverse A. From these records in Fig. 4 and the graph in Fig. 6, it can be demonstrated that the seismic waves in a sand layer near a small explosion have only two kinds of simple wave group, provided the observation is made in an area of a really uniform half-space.

Increase and diminution of wave energy

The amplitude of each peak and trough increases or diminishes regularly as the epicentral distance becomes longer, as can be seen in Figs. 3 and 4.

For example, the peak II-1U illustrated in Fig. 5 is predominant

near the shot point, but it shows fair decay around 7 m and at last it can hardly be seen in the vicinity of 9 m from the shot point. The trough II-1D which follows II-1U, has a longer life. It shows still considerable predominance around 8 m from the shot point, but it becomes weaker at 10 m and practically disappears around 12 m from the shot point. The trough II-2D can hardly be recognized just near the shot point. It comes in sight for the first time around 4 m and gains energy after that. Though its development reaches the climax at the point of 13~14 m, the trough returns to falling and at last shows a considerable decline in the vicinity of 18 m from the shot point. We find that the same rise and fall as in this case is seen in the other wave groups. The following description is the outline of the increase and diminution of wave energy about the second and the fourth wave groups.

Needless to say, we should pay attention to the existence of the following two unfavorable factors in the case of examining the aspect of the rise and fall of each peak or trough in a given wave group:—i) The error caused by the lack of uniform sensitivity of equipment in each trace. ii) The troubles caused by the fact that the wave generated by an explosion generally has a tendency to attenuate with the extension of the distance from the shot point.

In order to avoid the unfavorable influences caused by these disadvantages, we adopted the following simple methods. The procedure we took to get rid of the first factor was as follows. We concentrated the geophones at a point 30 m from the shot point to test whether each trace keeps uniform sensitivity. In the records thus obtained we read off the values of the amplitudes of the corresponding waves of all traces and then calculated the ratio of the value of each amplitude to the mean value of all the corresponding amplitudes. We regarded the value of the ratio for each trace as each relative sensitivity. Dividing the amplitude of each peak or trough by the corresponding relative sensitivity, we obtained the corrected amplitude.

After this procedure was performed for all amplitudes, the following procedure was taken to get rid of the second factor. We measured the corrected maximum amplitude of each group at respective distances. The relations between the maximum amplitudes thus obtained and the epicentral distance are illustrated in Figs. 7 and 8, which respectively correspond to the second and the fourth groups. Though we can find some disturbance at a great distance in each figure, a regularly logarithmic decrease of the maximum amplitude is seen in each group as

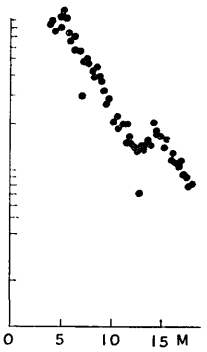

Fig. 7. Corrected maximum amplitude related to the epicentral distance for the second wave group.

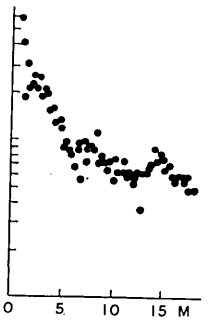

Fig. 8. Corrected maximum amplitude related to the epicentral distance for the fourth wave group.

the distance becomes longer. We calculated the values of the ratio of the corrected amplitude of each peak or trough to the corrected maximum amplitude with regard to each group at respective distances. Now we can know the aspects of the rise and fall of each peak or trough, because we believe we were able to take away the two unfavorable factors through the above procedures.

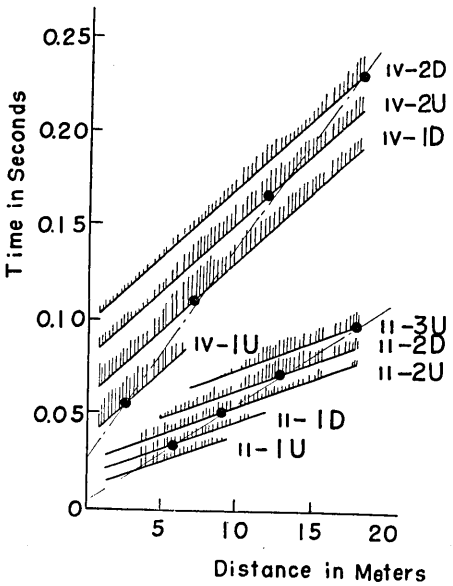

Fig. 9. Rise and fall of each peak ro trough related to the epicentral distance.

Fig. 9 shows the values of the amplitude ratios of the second and the fourth groups, which are drawn on the travel-time curves. The length of the bar is in proportion to the value. We can see clearly the rise and fall of each peak or trough. A wave appears, gains its energy gradually, reaches the climax of energy and after that it loses its energy and in the end disappears. The solid circles in the figure stand for the points where the energy of each peak or trough amounts to maximum. These solid circles of each group seem to stand in a chain line of

which the slope shows the minimum group velocity of the wave group, as K. Tazime[2] has pointed out. The values are 190 m/sec and 90 m/sec in the case of the second and the fourth groups respectively. Although the chain line of the second group starts from around the origin, that of the fourth group has a fairly great intercept time. This may be caused by the fact that, in the case of correcting the attenuation of the amplitude of the fourth group derived from the extension of distance, we used the disturbed curve illustrated in Fig. 8 as the standard. Therefore a question arises as to whether each solid circle illustrated in Fig. 9 stands for the maximum energy of each peak or trough of the fourth group or not. As can be seen in Fig. 8, the corrected maximum amplitudes which are used as the denominators of the ratios show greater value as expected in the vicinity of the distance a little farther from the solid circle on the peak IV-2U. So, we may suppose that the apparent energy of a wave at such distance seems to be smaller than it really is. The same question as this may arise in the case of IV-1U and IV-1D and so on. If we put in a strict correction in each case, the apparent slope of the chain line connecting every solid circle in Fig. 9 will pass near the origin. It represents a characteristic of a dispersive surface wave that the chain line whose slope shows the group velocity starts from the origin in the travel-time graph. From this criterion we conclude that the latter part of the second wave group and the fourth wave group are safe to be considered as surface waves.

Energy of wave groups

In order to classify the wave type of the wave groups, we investigated the aspect of the attenuation of energy of each wave group with regard to the epicentral distance.

We calculated the value of the wave energy by means of Howell's method[3], considering that the recorded amplitude represents the particle velocity. Under the assumption that the seismic energy does not spread radially but is confined to the vicinity of the surface plane and that the velocity of transmission is constant for the whole pulse, the energy flowing through a surface element of unit cross section which is perpendicular to a radial line at radius, R, is:

$$E=\frac{\rho c}{2}\sum v^2\Delta t\,,$$

2) K. TAZIME, *Journ. Physics of the Earth*, **4** (1956), 113.

3) B. H. HOWELL, Jr. and D. BUDENSTEIN, *Geophysics*, **XX** (1950), 33.

where ρ represents the density of the medium, v the particle velocity, c the velocity of propagation of the energy and Δt the element duration time of the energy. Furthermore, considering the attenuation caused by the viscosity and the solid friction, etc, the formula

$$e^{-\alpha X}=CX^{A}\Sigma v^{2}\Delta t$$

is obtained. Here α stands for the above mentioned rate of attenuation, and A represents the rate of attenuation concerning the distance X, and C is a constant. Between the results of the second and the fourth wave groups on Traverse A, the former proved to be not good. We got $A=1.0\pm0.3$ and $\alpha=0.16\pm0.05$/m regarding the fourth group. Therefore, we can guess the energy of the fourth group spreads in a way similar to the surface wave.

As for the energy of the body wave at Traverse B, we calculated the rate of attenuation of the perticle velocity β $(=\alpha/2)$ due to the viscosity, etc, at every spread applying the exponential equation

$$v=v_0X^{-1}e^{-\beta X}$$

to this case under the assumption that the rate of attenuation of the particle velocity as to the distance is 1. In Fig. 10 we plotted the values at every spread thus obtained as corresponding to the middle point of each spread. As can be seen in this figure, β becomes smaller with the extension of the distance from the shot point. Although this may be caused by the fact that we fixed the rate of attenuation regarding the distance as 1, it is possible that there are other causes.

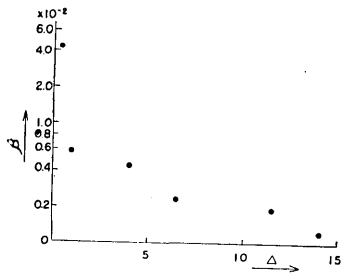

Fig. 10. Relation between the rate of attenuation β and the epicentral distance.

Orbit of ground motion

In order to obtain additional materials for the classification of the wave groups, it is a common procedure to check the orbit of the ground particles due to the seismic waves. In general, the orbit is examined by projecting an actual ground motion on a horizontal or on a vertical plane containing the seismic source and geophone.

In our measurements, however, we obtained the records of grounb velocity rather than of ground displacement. So the orbits of the particle velocity were drawn except at Traverse B. Fig. 11 shows examples of respective orbits of the second, the third and the fourth wave groups

which were obtained at Traverse A. At the same time, the figure shows the wave forms which were used in the case of drawing the orbits. Judging from the orbits, the second wave group consists of two parts. The first part shows a pull-push motion which is characteristic of a compressional wave. The succeeding part illustrates somewhat vertically polarized motion whose rotational direction is derect. The third group has a direct motion. This group seems to be a kind of typical hydrodynamic wave. H. Sima[4] obtained some reasonable results under the assumption this wave group was an M_{12} wave which was propagated through the surface layer of dry sand underlaid by the water-saturated sand layer. On the other hand, the fourth group shows a retrograde motion. It can be regarded as an ordinary Rayleigh-type wave.

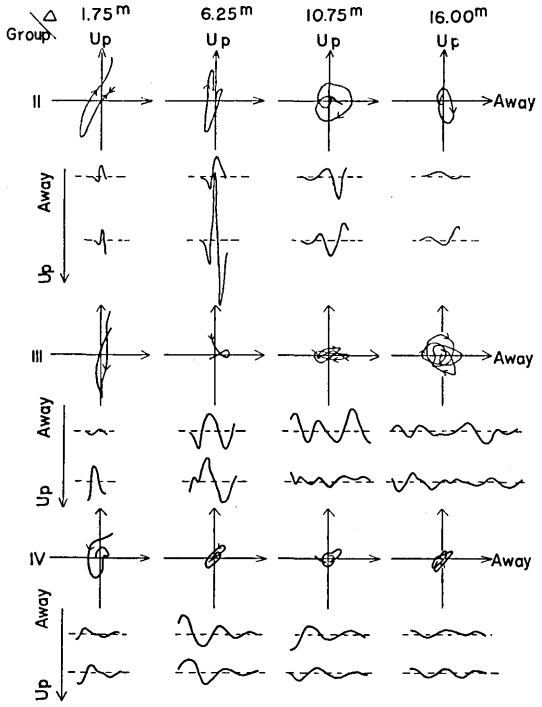

Fig. 11. Ground motion graphs for the second, the third and the fourth wave group at Traverse A.

We drew the orbits of the actual ground motions on the vertical plane concerning the surface wave at Traverse B. In this case, we obtained the displacement motions by means of integrating the records of the particle velocity according to Sympson's method. On the basis of the result, the particle displacement orbits were shown in Fig. 12. Strictly speaking, the shape of this orbit will be generally different from that of the velocity orbit of the ground motion, because the higher frequency components of ground motion have a greater influence on a velocity orbit than on a displacement

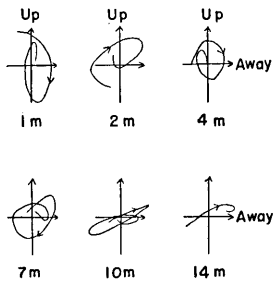

Fig. 12. Ground motion graphs for the surface wave at Traverse B.

4) H. SIMA, *Rep. Seis. Exp. Group of Japan*, **11** (1956), 30, (in Japanese).

orbit. But there will hardly be any difference in a direction of motion between these two orbits. Therefore, we may inquire into the relation between the direction of motion of the velocity orbits at Traverse A and that of the displacement graphs at Traverse B. As can be seen in Fig. 12, this surface wave shows a direct motion and it resembles the third wave group at Traverse A. Hence, the third wave group at Traverse A may be regarded as a wave group connected with the lower layer soaked in sea water.

The orbits of the particle velocity at Traverse C were drawn directly from the observation records, as shown in Fig. 13. The same retrograde orbits as of the fourth group at Traverse A are seen in this case. Therefore, the fourth wave group may be considered as a surface wave group that is related to the upper layer of dry sand.

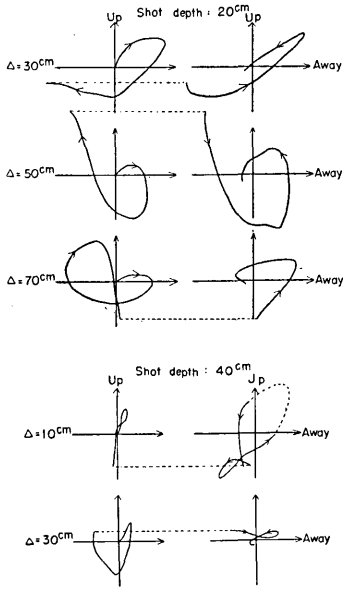

Fig. 13. Ground motion graphs for the surface wave at Traverse C.

S phase

From these vertical observation records, as in any other case of explosion seismic experiments, there can be seen no phase which can be regarded as an S phase. On the other hand, as will be seen from the transverse records in Fig. 14, that were obtained at Traverse A and arranged in order of epicentral distance, we can trace a series of distinct arrivals of the events which seem to have characteristics of an S wave. Plotting these arrivals, we obtain the two segments of travel-time curves of different phases which give velocities of 140 m/sec and 340 m/sec respectively as shown in Fig. 15. Judging from the values of the velocities, the former seems to represent the S wave corresponding to the P wave having a velocity of 245 m/sec. As for the latter, when we take into consideration the fact that the substratum is saturated with sea water, it still remains somewhat difficult to call it the S wave that corresponds to the P wave having a velocity of 1400 m/sec. However, the depth of the interface between the superficial layer and the substratum, calculated from the time-distance graph, gives a value of

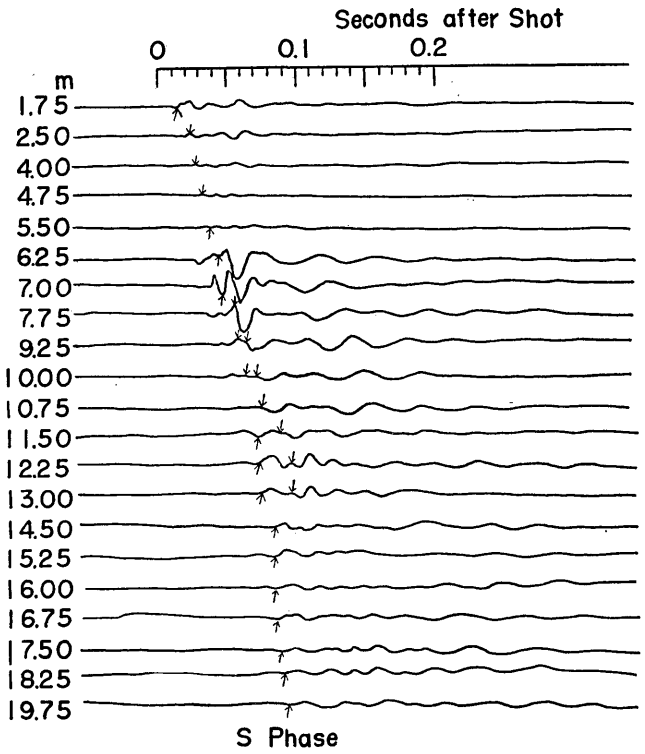

Fig. 14. *S* phases observed on the transverse horizontal geophones along Traverse A.

about 2.6 m, which is in good accord with the value of the depth calculated from *P* wave. This may serve as a positive base for the claim of the *S* wave for the latter segment. We calculated also the Poisson's ratio of the superficial layer of dry sand and of the substratum of wet sand. Their values are about 0.26 and 0.47 respectively. From the fact that the density of the upper layer medium is 1.64 gm/cc, we obtained its rigidity as about 3.2×10^8 dyne/cm^2 and its Lamé's constant as about 3.4×10^8 dyne/cm^2.

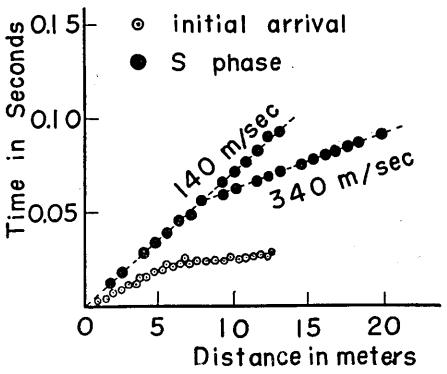

Fig. 15. Travel-time curves of *S* phase.

Conclusion

In the observations on the ground where one uniform layer is underlaid by a uniform half space, it was confirmed there are four types of wave group. Of these four wave groups, the first one is the bodily P wave propagated through the substratum. The second one consists of the P wave and a kind of surface wave following it, which are propagated together through the superficial layer. The third and the fourth groups are regarded as the surface waves corresponding respectively to a kind of hydrodynamic wave and to the ordinary Rayleigh wave. The third group is considered by H. Sima to represent the M_{12} wave that can exist in the surface solid layer underlaid by the sand layer soaked in sea water.

In the observations on the further simple ground which had a structure of an ideal uniform half space, we succeeded in obtaining much simpler records. In these records, only two kinds of wave group were observed, i.e. the bodily P wave and the surface wave. The surface wave, however, was not the ordinary type of Rayleigh wave that was expected from the elastic theory of seismic waves, because the medium was so much saturated with sea water.

Moreover, we found phases which seemed to be characteristic of an S wave. They are regarded as the S waves propagated through the superficial layer and through the substratum respectively.

Acknowledgements

The authors are very grateful to the Japan Petroleum Exploration Co. Ltd. for their hearty cooperation in these experiments. Their thanks are due to the Seismic Exploration Group of Japan headed by K. Sassa. They further wish to thank Assistant Professor G. Miki of the Institute of Industrial Science in the University of Tokyo, for testing the grain-size distribution of the sand of the field. A part of the expenses necessary for these experiments was defrayed from the funds for scientific research of the Ministry of Education, for which the authors here express their gratitude.

17. 砂層の中を伝わる波の波形について

地震研究所 表 俊一郎
小牧昭三
中島直吉(旧姓小林)

実験室内の模型実験に於て観測される弾性波と自然地震に於て観測される波とを結びつけるものとして，簡単な地下構造の地域で小量の火薬爆発によつて起される波の発生及び伝播の有様を研究することは，複雑な条件の下に発生する自然地震の震動現象を理解する上に有用と思われる．

上の如き目的のために，1955 年と 1956 年の 2 回にわたり一様均質と考えられる砂層より成る，新潟県潟町の砂浜に於て小爆破実験を行つた．

1955 年には汀線より 20 m 程離れた所に測線を設けたが，地下約 3 m の所に海水の浸入による不連続面があり，そのために得られた記録は期待した程簡単でなく 4 つの波群に区分された．1956 年には，より簡単な記録を得るために汀線に測線を設けて観測を行つた．この場合は実体波と表面波とからなる簡単な記録が得られた．位相速度，energy の減衰，ground motion の orbit を調べた結果，この実体波は 1955 年の観測で得られた記録における第 1 波群，表面波は第 3 波群に対応することが大体解つた．而して，第 1 波群は含水砂層を伝わる実体波であり，第 2 波群は乾いた砂層を伝わる実体波と，それに続く表面波とより成る．第 3 波群は direct motion をする表面波で hydrodynamic wave の一種と見做される．また第 4 波群は retrograde motion を示し Raylaigh 型の表面波と解される．

また得られた記録は簡単で而も，PU. を 25 cm 間隔において観測されているために波の消長の有様をしらべるのに適している．早く現われる山または谷は，shot point 近くでその振巾，即ち波の energy は既に大きくて，距離と共に減少の一途を辿り消え失せるが，遅く現われるものは，次第に成長して最大振巾に達し，その後減退して行く．而して走時曲線において一連の山または谷が最大振巾に達する点は各波群毎に一直線上に大体載つており，その直線は origin を通る．これらの直線の傾斜は夫々の波群の群速度を示していると考えられる．

更に，1955 年に於ける観測の Transverse の記録より S 波らしい phase を読み取ることが出来た．走時曲線を描くと 140 m/sec, 340 m/sec を示す二つの分枝が得られ，これは夫々砂層及び含水砂層を伝わる S 波と考えられる．これより両層の境界面の深さを求めると P 波から求められた境界面の深さと殆んど一致する値が得られた．これら P, S 両波の速度から砂層の弾性常数も求めた．